HHS Public Access

Author manuscript

Surg Endosc. Author manuscript; available in PMC 2018 January 01.

Published in final edited form as:

Surg Endosc. 2017 January ; 31(1): 477–486. doi:10.1007/s00464-016-4936-4.

A Novel Retractable Laparoscopic Device for Mapping Gastrointestinal Slow Wave Propagation Patterns

Rachel Berry, MPhil[1], **Niranchan Paskaranandavadivel, PhD**[1], **Peng Du, PhD**[1], **Mark L Trew, PhD**[1], **Gregory O'Grady, FRACS**[1,2], **John A Windsor, FRACS**[2], and **Leo K Cheng, PhD**[1,3]

[1]Auckland Bioengineering Institute, University of Auckland, Private Bag 92019, Auckland 1142, New Zealand [2]Dept. of Surgery, University of Auckland, New Zealand [3]Dept. of Surgery, Vanderbilt University, TN, USA

Abstract

Background—Gastric slow waves regulate peristalsis, and gastric dysrhythmias have been implicated in functional motility disorders. To accurately define slow wave patterns, it is currently necessary to collect high-resolution serosal recordings during open surgery. We therefore developed a novel gastric slow wave mapping device for use during laparoscopic procedures.

Methods—The device consists of a retractable catheter constructed of a flexible nitinol core coated with Pebax. Once deployed through a 5 mm laparoscopic port, the spiral head is revealed with 32 electrodes at 5 mm intervals. Recordings were validated against a reference electrode array in pigs and tested in a human patient.

Results—Recordings from the device and a reference array in pigs were identical in frequency (2.6 cycles per minute; p=0.91), and activation patterns and velocities were consistent (8.9±0.2 vs 8.7±0.1 mm s^{-1}; p=0.2). Device and reference amplitudes were comparable (1.3±0.1 vs 1.4±0.1 mV; p=0.4), though the device signal to noise ratio (SNR) was higher (17.5±0.6 vs 12.8±0.6 dB; P<0.0001). In the human patient, corpus slow waves were recorded and mapped (frequency 2.7±0.03 cycles per minute, amplitude 0.8±0.4 mV, velocity 2.3±0.9 mm s^{-1}).

Conclusion—In conclusion, the novel laparoscopic device achieves high-quality serosal slow wave recordings. It can be used for laparoscopic diagnostic studies to document slow wave patterns in patients with gastric motility disorders.

Keywords

Gastric electrical activity; gastric dysrhythmia; high-resolution mapping; nitinol

Corresponding Author. Associate Professor Leo Cheng, Auckland Bioengineering Institute, University of Auckland, Private Bag 92019, Auckland 1142 New Zealand, Tel: +64 9 373 7599; fax: +64 9 367 7157; l.cheng@auckland.ac.nz.

Disclosures

RB, MT and JW report no conflict of interest or financial ties to disclose.

1. Introduction

Gastric contractions are coordinated by an underlying electrical activity, termed slow waves, that are generated and propagated by the interstitial cells of Cajal (ICC) [1]. In the human stomach, slow waves originate from the pacemaker region situated in the mid/upper corpus on the greater curvature, and propagate antegrade towards the pylorus at a frequency of approximately 3 cycles per minute (cpm) [2, 3].

Abnormalities of slow wave activity, termed gastric dysrhythmias, are associated with common and highly symptomatic disorders including gastroparesis, functional dyspepsia and may also play a role in the acute or chronic delayed gastric emptying observed after some gastrointestinal (GI) surgical procedures [4–6]. However, the clinical significance of gastric dysrhythmias has been unclear, principally because past data was accumulated using sparse serosal or cutaneous recordings [7]. One such method is electrogastrography (EGG) which involves placing cutaneous electrodes on the abdomen in a manner similar to electrocardiography. EGG, while able to show variations in frequency or rhythm that may be associated with a dysrhythmia, cannot provide the spatiotemporal detail required to quantify and reliably classify normal and abnormal propagation patterns [7–10]. To reliably assess propagation patterns, bioelectrical potentials must be recorded directly from the tissue surface, preferably using a 2D array of closely spaced electrodes [8, 9].

To date, relatively little data has been collected during clinical studies and the clinical significance of slow wave dysrhythmias therefore remains poorly defined. To overcome this problem, high-resolution (HR) multi-electrode mapping has been adapted from cardiac electrophysiology as a more accurate method of defining gastric dysrhythmias in spatiotemporal detail [11, 12]. To date, HR mapping studies in humans and animals have been performed using custom-built silver-wire electrode arrays and flexible printed circuit board electrode arrays [13, 14]. Although these methods are able to accurately define gastric dysrhythmias, they require recordings to be taken directly from the serosal surface of the GI tract using relatively large electrode platforms and cabling, limiting their application to invasive open-abdominal surgery [2].

The adoption of minimally invasive surgical procedures for the treatment of GI diseases continues to expand. Consequently, it is essential to develop new laparoscopic devices for minimally invasive recording of slow wave activity directly from the serosal surface of the GI tract, facilitating future targeted treatment for dysrhythmias [15]. However, current laparoscopic approaches record from a limited number of electrodes covering a small spatial area (approximately 4×4 mm^2) [15, 16]. It is necessary to record from a larger field of electrodes to accurately define dysrhythmias and to avoid large errors when estimating the direction and velocity of slow waves [7]. An improved approach would allow reliable, high-quality multi-channel recordings over a larger portion of the serosa, be deployable through a 5 mm laparoscopic port, and preferably allow repeat sterilization for human use [17].

This study presents the design and validation of a novel laparoscopic device capable of accurately recording slow wave activity, including complex dysrhythmias, in HR spatiotemporal detail.

2. Materials and Methods

Design and Fabrication

The novel laparoscopic device is shown in Figure 1, together with the reference electrodes used for validation [13]. The device consists of a retractable catheter embedded with 32 electrodes, a rigid introducer sheath, and a flexible connecting cable. The device was designed to be deployable and retractable through a 5 mm laparoscopic port, for placement against the serosal surface of the GI tract without the need for attachment by suturing or clipping. It is sterilizible using low-temperature hydrogen peroxide sterilization techniques such as STERRAD (Advanced Sterilization Products), V-PRO® maX (STERIS) or ethylene oxide [17, 18]. Fabrication was performed by Access Point Technologies (APT, Rogers, MN, USA).

The retractable catheter (diameter 2.2 mm, length 330 mm) was constructed of nitinol wire with a Pebax® coating. Nitinol is a nickel-titanium alloy widely used in expandable medical devices, including cardiac mapping devices, due to its favorable elastic and shape-memory properties [19, 20]. Pebax® is a thermoplastic elastomer consisting of polyamide and polyether segments, and was favored as it is light-weight yet strong, waterproof, highly flexible and readily deformable, while being suitable for sterilization and compliant with US Pharmocopeial Convention Class VI Reference Standards [21]. Individual electrodes were fabricated in platinum (90%) and iridium (10%), because this has been successfully applied previously to study electrical activity in the GI tract [22]. The Pebax® coating was exposed in 32 locations, spaced 5 mm apart to reveal the 32 ring electrodes of 1 mm width. This electrode spacing and arrangement allowed dysrhythmic slow wave activity to be captured based on experiences in previous studies [23].

A nylon outer sheath, (sized to pass freely through a 5 mm laparoscopic port) was used to house and introduce the mapping catheter. The catheter was designed to deploy through this sheath, and once free of the sheath, to form into a spiral arrangement (diameter 30 mm at full extension) (Figure 1A). The catheter was designed to be readily retracted into the outer sheath, aided by the flared end (Figure 1B). The shaft of the device was fabricated of stainless steel. At the end of the catheter, the connecting wires were routed through a 1.5 m flexible cable to an acquisition system outside the sterile field.

Porcine Validation Trials

The device was validated *in-vivo* by comparison to reference recordings from an established experimental model in healthy white cross-breed weaner pigs (n=5, mean weight 34.2 ± 1.9 kg) [24]. Ethical approval was obtained from the University of Auckland Animal Ethics Committee. The reference electrode arrays were validated recording platforms with gold-tipped electrodes arranged in a grid configuration at an inter-electrode spacing of 4–5 mm (Figure 1C,D) [13]. The animals were fasted overnight, then subjected to general anesthesia with Zoletil (Tiletamine HCl 50 mg/ml and Zolazepam HCl 50 mg/ml), followed by isoflurane (2.5 – 5 % with an oxygen flow of 400 mL within a closed circuit anesthetic system). Vital signs were continuously monitored and maintained, and body temperature

was kept in the normal physiological range using a heading pad. The animals were euthanized while still under anesthesia via a bolus injection of 50 ml of magnesium sulphate.

A midline laparotomy was performed exposing the anterior gastric serosal surface. The reference electrodes and laparoscopic device were gently placed on the serosal surface of the stomach with minimal handling of the viscera. Ground electrodes were positioned on the lower abdomen and hindquarter thigh. The reference electrodes were maintained in position by using warm saline-soaked gauze packs, and the laparoscopic device was held steady in position, to reduce movement artifacts. The incision site was also covered with warm soaked packing to prevent cooling of the abdominal cavity and gastric serosa. A period of stabilization was allowed before recording. In all studies (including the human trials), the stomach was not distended, as over-distention of the stomach may invoke slow wave changes including dysrhythmias [25, 26].

Human Trials

On completion of validation in the porcine model, a human trial was conducted with a separate sterilized laparoscopic device for validation in an intra-operative environment. Ethical approval was obtained from the Northern Y Health and Disability Ethics Committee. With informed consent, the study was performed on a 53-year-old male undergoing a routine laparoscopic anti-reflux surgery at Auckland City Hospital.

No restrictions were placed on the anesthetic protocol for this patient. General anesthesia does not have a significant impact on slow waves [10, 14], and existing descriptions of human gastric slow wave activity are also derived from studies performed under an anesthesia [2, 3]. Administered agents included a rapid-acting opiate, a muscle relaxant, propofol, and sevoflurane.

Following anesthetic induction, intubation, insertion of laparoscopic ports and abdominal insufflation, but prior to tissue dissection or mobilization, the device was deployed into the abdominal cavity via a 5 mm trochar adjacent to the xiphisternum, and placed on the anterior serosal surface of the distal corpus. The device was manually held in position and steadied against the laparoscopic port. The recording apparatus was set up as previously described, with reference electrodes placed on the shoulders [2, 15]. Signal acquisition and quality was assessed by quantifying amplitude, velocity and frequency of slow wave events and the signal to noise ratio (SNR), in comparison with previous benchmarks [15, 27].

Signal Acquisition and Analysis

Signals were acquired using an ActiveTwo System (Biosemi, Amsterdam, Netherlands) modified for passive electrode recordings. Data was acquired at 512 Hz. Signal processing was conducted offline in the Gastrointestinal Electrical Mapping Suite (GEMS) v1.5 [28]. Data were filtered using a Gaussian moving median filter (20 s moving window) and a Savitzky-Golay filter (window 1.7 s, polynomial order 9) [29]. Slow wave activation times were calculated, and activation maps generated, using established algorithms followed by manual review and correction [30, 31]. SNR was calculated by dividing slow wave recordings into signal and noise dominated segmented based on activation times. A three

second window was placed around the slow wave activation time and defined as the signal vector, while the remaining segments were classified as the noise vector,

$$SNR=20\ \log_{10}10\left(\frac{\mathrm{RMS(signal\ \ vector)}}{\mathrm{RMS(Noise\ \ vector)}}\right)$$

where RMS is the root mean square [32]. Slow wave amplitudes were calculated by applying a peak-to-trough detection algorithm based on the 'zero-crossing' of the first- and second-order signal derivatives of each slow wave event [33]. The velocity vectors for the reference electrode array were calculated using a finite difference method with a Gaussian smoothing filter [34]. As a result of the irregular arrangement of the electrodes in the laparoscopic device, the velocity was estimated using a second order polynomial fit of the activation time wavefront [35, 36],

$$T(x,y)=a.xy+b.x+c.y+d,$$

where *T(x,y)* is the activation time wavefront in the *x* and *y* positions, while *a, b*, *c* and *d* are the coefficients of the equation. Compared to the previous laparoscopic recording electrode design [15], the spatially distributed 32 electrodes of the spiral electrode provide a more robust estimation of activation direction and activation time gradients for determining conduction velocity. Furthermore, the 32 electrodes enable channels with poor signal quality to be discarded from the analysis without compromising confidence in the predictions. In contrast, poor recordings in one channel of a previous laparoscopic mapping device [15] may severely compromised estimates of slow wave orientation and velocity. All recordings were screened for signs of dysrhythmic activity; defined as any deviation from organized, regular slow wave propagation in an aboral direction, including all propagation pattern, frequency, or direction compared with known normal data [24, 37].

Statistical Methods

All statistical analyses were performed in IBM SPSS Statistics v20.0. Slow-wave frequencies, velocities and amplitudes are presented as means ± standard error of the mean (SEM) unless otherwise specified. A Student's t-test or one-way ANOVA with Tukey' post-test were used to analyze statistical differences, with $P < 0.05$ regarded as significant.

3. Results

Porcine Validation Trial

Gastric slow-wave activity was successfully recorded simultaneously via both the novel laparoscopic device and the reference array in all five porcine trials. The recording period totaled 105 minutes (mean 15.1 ± 5.1 minutes) over the five experiments.

A representative example of gastric slow wave events recorded over a 90 second period by both the laparoscopic electrode in five channels, and the reference electrodes in six channels, are shown in Figure 2. Both the laparoscopic and reference electrodes achieved high-quality slow wave signals. Signal morphology was comparable between the arrays, and the events

were concordant with known extracellular slow wave characteristics, including biphasic potential pattern, downstroke rate and width [37]. The mean frequency of slow wave activity across the pigs was 2.6 ± 0.4 cycles per minute (cpm) and within the known physiological range for the porcine stomach [24]. Frequency and amplitude was comparable between recording methods (2.5 ± 0.4 cpm vs 2.6 ± 0.4 cpm; $p = 0.91$; 1.3 ± 0.1 mV vs 1.4 ± 0.1 mV; $p = 0.4$). However, the laparoscopic device was found to have a higher SNR than the reference electrodes (7.5 ± 0.6 dB vs 12.8 ± 0.6; P<0.0001), due to reduced noise of the baseline signal from which the slow waves were identified.

Slow wave activation times were calculated from the slow wave events, as demonstrated in Figure 2, and used to generate activation maps, as shown in Figure 3. These maps demonstrate the propagation of activity in an aboral direction in both the laparoscopic device and the reference electrodes.

Figure 3 also demonstrates example velocity and amplitude maps for both the laparoscopic device and the reference electrodes, with propagation again in an aboral direction. Table 1 reports the difference in mean frequencies, amplitudes, SNR and velocities between the laparoscopic device and reference electrode for all five porcine trials. Recorded slow wave velocities were comparable between the laparoscopic device and the reference electrodes (8.9 ± 0.2 mm s^{-1} vs 8.7 ± 0.1 mm s^{-1}; $p = 0.2$).

Dysrhythmic activity was observed in one of the pigs in the form of a deviation in direction from aboral, to circumferential, to orad (Figure 4). This dysrhythmic pattern suggested a shifting ectopic pacemaker of the type known to occur in the acute weaner pig model used in this study [10].

Human Intraoperative Trial

Following successful trials in the porcine model, another sterilized laparoscopic device was used for human intraoperative validation. The retractable catheter was readily deployed and withdrawn through the 5 mm laparoscopic port and manually held in position on the serosal surface of the stomach (see Figure 5). Prior to tissue dissection and with minimal organ handling, slow wave activity was recorded over a period of five minutes from the mid corpus, close to the angularis incisura. An example of three slow wave events from three channels of the laparoscopic device is shown in Figure 5.

Signal morphology was of high-quality, and slow wave events were concordant with known extracellular slow wave characteristics, including the biphasic potential pattern, downstroke rate and width [37]. Mean amplitude was 0.8 ± 0.4 mV [2]. Slow wave activity was recorded at a frequency of 2.7 ± 0.03 cpm, which is within the known physiological range for human gastric slow waves [3, 38]. Recorded velocities were also within the known physiological range for human gastric slow waves in the mid-corpus region (2.3 ± 0.9 mm s^{-1}) [2]. Activation times calculated from slow wave events are illustrated in Figure 5. This image demonstrates the aboral propagation of slow wave activity.

4. Discussion

This study introduces a novel retractable laparoscopic device for mapping GI slow wave propagation patterns. The device can withstand multiple sterilization processes and the flexible spiral head has been designed to deploy through a 5 mm laparoscopic port. The most accurate technique for determining the spatiotemporal properties of slow waves is HR mapping, typically involving the placement of an array of recording electrodes (often >100) on the serosal surface of the organ of interest [8, 13]. Although ideal, this approach requires direct serosal access and had therefore been restricted to operations involving large incisions. The device detailed in this study overcomes this issue by enabling laparoscopic HR slow wave data capture over a larger area.

The device now offers the opportunity to characterize both normal and altered bioelectrical potentials in patients undergoing routine laparoscopic procedures. The first major application will be in studies continuing to elucidate fundamental human GI electrophysiology, including investigating slow wave activation and recovery profiles throughout the GI tract, pacemaker behavior, anisotropic conduction dynamics and responses to electrical stimulation therapies (e.g. [2, 39]). In addition, the device can be used in the investigation of patients suffering motility disorders such as gastroparesis and chronic unexplained nausea and vomiting, where dysrhythmias are strongly implicated [7, 9, 25]. Lastly, the device will be particularly valuable in defining the role of disordered electrical activity in delayed recovery after surgical procedures, such as gastrectomies, gastric excisions, fundoplication or bariatric surgery, where slow wave conduction pathways are altered or disrupted [40]. Until now, accurate research on these subjects has been limited due to lack of mapping technologies.

Validation was performed in a porcine model by comparing data collected using the laparoscopic device with that from a standard reference electrode in common current use [13]. It achieved high-quality slow wave recordings that surpassed the reference electrode in SNR, and was shown to be capable of accurately measuring the direction, amplitude, velocity and activation times of slow wave activity, including dysrhythmic episodes. The device also enabled intra-operative laparoscopic human mapping, successfully achieving recordings in the operating room.

This device has been designed specifically for mapping slow wave activity during laparoscopic procedures. It has a number of design features that distinguish it from more traditional arrays [13], and improves on previously described laparoscopic devices [15, 16]. The major developments in this novel design are concentrated on the recording head. Its flexibility permits easy deployment and retraction through a 5 mm laparoscopic port, and the recording area covered is increased on a previously described device (707 mm^2 vs 13 mm^2) [15]. The superior size allows for incorporation of a greater number of recording channels (32 vs 4), resulting in substantially greater data acquisition from the target organ. This in turn increases accuracy of slow wave velocity and activation sequence calculations, and the probability of detecting dysrhythmias. It also increases the likelihood of achieving a quality recording in one or more channels if other channels are affected by signal artifact or poor contact. Alternative designs, such as linear arrangements of electrodes or smaller arrays

would be easier to construct and apply, however, it is now clear that achieving high-resolution wide-area coverage enables optimal data retrieval for detecting and classifying dysrhythmic events, as well as to define the velocity and amplitude changes that accompany dysrhythmias [40].

The manual positioning of the device has eliminated the requirement for suturing or clipping, and the smooth, flexible design of the recording head minimizes the risk of tissue damage or organ perforation. It is composed of materials that allow for sterilization to the level of other surgical equipment, and reuse over several studies. Pebax® is capable of withstanding Sterrad® and V-PRO® sterilization, unlike other polymer materials that may suffer damage [41].

The deformable structure of the recording head is not only essential for deployment and retraction through a laparoscopic port, but also adapts to the curvature of the stomach, thus improving contact between the recording channels and the surface of the organ. However, the trade-off in design is that this flexibility also contributes to variation in the proximity and spatial positioning of the recording channels during data collection, and therefore could contribute to errors in the estimation of slow wave velocities. This error may also be accentuated by inconsistencies in the size and shape of recording channels resulting from the hand-made nature of the device. Nevertheless, our validation studies showed acceptable accuracy in velocity compared to established standard recording techniques [13], so the device does provide accurate spatiotemporal knowledge regarding the direction and velocity of slow wave propagation at the point of measurement. Results also suggest that movement artifacts associated with the design of the device were not significant, if attention is paid to device handling and deployment, and signal quality remains high.

Based on previous investigations, slow wave recordings are considered to be stable under anesthetized conditions [2, 3, 10, 37]; therefore, the laparoscopic device is expected to achieve reliable slow wave data. Dysrhythmic activity has been described previously under the influence of opiates, however, small doses of rapid acting opiates, as used in this study, appears to have minimal impact on slow wave patterns at the time of mapping [2].

Currently, the impact of surgery on slow waves propagation is uncertain because past methods have applied sparse electrode coverage, whereas high-resolution mapping is required to accurately define and classify slow wave propagation patterns [2, 9]. Investigation of the relationship between slow wave characteristics (amplitude, velocity, and frequency, and direction of propagation) and post-surgical symptoms could provide a substantially improved understanding of the role of bioelectrical disturbances in post-operative gastric dysmotility. With future advances, the device could also be useful for the targeted investigation and therapy of gastric dysrhythmias, which underlie significant gastric motility disorders, such as gastroparesis and chronic unexplained nausea and vomiting [9, 25].

This design is a compromise between invasiveness and spatiotemporal recording quality. The most widely employed non-invasive technique for gastric electrical disorders is electrogastrography (EGG) [42], but this approach is currently unable to provide the

spatiotemporal detail required to quantify and reliably classify slow wave propagation patterns [7]. Magnetogastrography (MGG) is another non-invasive technique, which records the magnetic field associated with slow wave propagation via a Superconducting Quantum Interference Device (SQUID) [43]. This method, however, is expensive, highly specialized, and only available to a limited number of researchers. It is also considered to be in its experimental stages [44].

A promising recent development is the design of a wireless implantable recording device that transmits slow wave recordings directly to analytical equipment, without the need for cables [45]. This system has the advantage that it may potentially be implanted allowing longer-term longitudinal studies without the increased potential for infection that wires traversing the abdomen may cause. It may also be applied in conjunction with an endoscopically implantable telemetry device that will allow continuous monitoring of slow wave activity in patients over a prolonged period of time, and in both fed and fasted states. Prototype implantable devices have been developed and tested in animal models, but further research is required before these are considered safe for human application [46].

This novel laparoscopic device provides another method for measuring slow wave activity. The device has been validated in both the porcine model and human subjects. It can withstand multiple sterilization processes and the flexible head has been designed to deploy through a 5mm laparoscopic port. The device is capable of accurately measuring the direction, amplitude, velocity and activation time of slow waves, and can also be used to map dysrhythmic activity. In conclusion, the design of this novel laparoscopic device will allow monitoring of slow wave activity in greater spatiotemporal detail during minimally invasive surgery than existing laparoscopic devices. The device will be a valuable asset for facilitating new laparoscopic clinical investigations of normal and dysrhythmic slow wave activity. In particular, it could be used for diagnosing dysmotility disorders and defining the effects of GI surgical procedures on bioelectrical potentials.

Acknowledgments

The authors gratefully acknowledge the assistance of Tim Angeli, Ryash Vather, Linley Nisbet, Grant Beban, and the surgical staff at Auckland City Hospital with data collection.

This work was supported in part by grants from the International Foundation for Functional Gastrointestinal Disorders (IFFGD), Maurice and Phyllis Paykel Trust (MPPT), Health Research Council of New Zealand, NIH (R01 DK64775), and Medical Technologies Centre of Research Excellence (MedTech CoRE), New Zealand. RB was supported by a Commonwealth Scholarship, PD by the Marsden Fund and LC by a Fraunhofer-Bessel Research Award from the Alexander von Humboldt Foundation and the Fraunhofer IPA.

NP, PD, GO and LKC hold intellectual property and/or patent applications in the field of mapping gastrointestinal electrophysiology.

References

1. Farrugia G. Interstitial cells of Cajal in health and disease. Neurogastroenterol Motil. 2008; 20:54–63. [PubMed: 18402642]
2. O'Grady G, Du P, Cheng LK, Egbuji JU, Lammers WJEP, Windsor JA, Pullan AJ. The origin and propagation of human gastric slow-wave activity defined by high-resolution mapping. Am J Physiol Gastrointest Liver Physiol. 2010; 299:G585–G592. [PubMed: 20595620]

3. Hinder RA, Kelly KA. Human gastric pacesetter potential - site of origin, spread, and response to gastric transection and proximal gastric vagotomy. Am J Surg. 1977; 133:29–33. [PubMed: 835775]
4. Lin X, Chen JZ. Abnormal gastric slow waves in patients with functional dyspepsia assessed by multichannel electrogastrography. Am J Physiol Gastrointest Liver Physiol. 2001; 280:G1370–G1375. [PubMed: 11352832]
5. Chen JD, Schirmer BD, McCallum RW. Serosal and cutaneous recordings of gastric myoelectrical activity in patients with gastroparesis. Am J Physiol. 1994; 266:G90–G98. [PubMed: 8304462]
6. Hocking MP, Harrison WD, Sninsky CA. Gastric dysrhythmias following pylorus-preserving pancreaticoduodenectomy. Dig Dis Sci. 1990; 35:1226–1230. [PubMed: 2209290]
7. O'Grady G, Wang THH, Du P, Angeli T, Lammers WJEP, Cheng LK. Recent progress in gastric arrhythmia: pathophysiology, clinical significance and future horizons. Clin Exp Pharmacol Physiol. 2014; 41:854–862. [PubMed: 25115692]
8. Lammers WJEP, Ver Donck L, Stephen B, Smets D, Schuurkes JAJ. Focal activities and re-entrant propagations as mechanisms of gastric tachyarrhythmias. Gastroenterology. 2008; 135:1601–1611. [PubMed: 18713627]
9. O'Grady G, Angeli TR, Du P, Lahr C, Lammers WJEP, Windsor JA, Abell TL, Farrugia G, Pullan AJ, Cheng LK. Abnormal initiation and conduction of slow-wave activity in gastroparesis, defined by high-resolution electrical mapping. Gastroenterology. 2012; 143(3):589–598. e1–e3. [PubMed: 22643349]
10. O'Grady G, Egbuji JU, Du P, Lammers WJ, Cheng LK, Windsor JA, Pullan AJ. High-resolution spatial analysis of slow wave initiation and conduction in porcine gastric dysrhythmia. Neurogastroenterol Motil. 2011; 23:e345–e355. [PubMed: 21714831]
11. Lammers WJEP. Arrhythmias in the gut. Neurogastroenterol Motil. 2013; 25:353–357. [PubMed: 23490042]
12. Cheng LK, Du P, O'Grady G. Mapping and modeling gastrointestinal bioelectricity: from engineering bench to bedside. Physiology (Bethesda). 2013; 28(5):310–317. [PubMed: 23997190]
13. Du P, O'Grady G, Egbuji JU, Lammers WJ, Budgett D, Nielsen P, Windsor JA, Pullan AJ, Cheng LK. High-resolution mapping of in vivo gastrointestinal slow wave activity using flexible printed circuit board electrodes: methodology and validation. Ann Biomed Eng. 2009; 37:839–846. [PubMed: 19224368]
14. Lammers WJ, Ver Donck L, Stephen B, Smets D, Schuurkes JA. Origin and propagation of the slow wave in the canine stomach: the outlines of a gastric conduction system. Am J Physiol Gastrointest Liver Physiol. 2009; 296(6):G1200–G1210. [PubMed: 19359425]
15. O'Grady G, Du P, Egbuji JU, Lammers WJEP, Wahab A, Pullan AJ, Cheng LK, Windsor JA. A novel laparoscopic device for measuring gastrointestinal slow-wave activity. Surg Endosc. 2009; 23:2842–2848. [PubMed: 19466491]
16. Familoni BO, Abell T, Voeller G. Measurement of gastric and small bowel electrical acivity at laparoscopy. J Laparoendosc Surg. 1994; 4:325–332. [PubMed: 7833517]
17. Thierry B, Tabrizian M, Trepanier C, Savadogo O, Yahia LH. Effect of surface treatment and sterilization processes on the corrosion behavior of NiTi shape memory alloy. J Biomed Mater Res. 2000; 51:685–693. [PubMed: 10880117]
18. Feldman LA, Hui H. Compatibility of medical devices and materials with low-temperature H2O2 gas plasma. Med Device Diagn Ind. 1997; 19:77–63.
19. Eldar M, Ohad DG, Goldberger JJ, Rotstein Z, Hsu S, Swanson DK, Greenspon AJ. Transcutaneous multielectrode basket catheter for endocardial mapping and ablation of ventricular tachycardia in the pig. Circulation. 1997; 96:2430–2437. [PubMed: 9337220]
20. Schmitt C, Zrenner B, Schneider M, Karch M, Ndrepepa G, Deisenhofer I, Weyerbrock S, Schreieck J, Schömig A. Clinical experience with a novel multielectrode basket catheter in right atrial tachycardias. Circulation. 1999; 99:2414–2422. [PubMed: 10318663]
21. Arkema Group Pebax® by Arkema. Arkema.
22. Cote KR, Gill RC. Development of a platinized platinum/iridium electrode for use in vitro. Ann Biomed Eng. 1987; 15:419–426. [PubMed: 3688577]

23. O'Grady, G.; Angeli, T.; Lammers, WJ. The principles and practice of gastrointestinal high-resolution mapping. In: Cheng, LK.; Farrugia, G.; Pullan, AJ., editors. New Advances in Gastrointestinal Motility Research. New York: Springer; 2013. p. 51-69.
24. Egbuji J, O'Grady G, Du P. Origin, propagation and regional characteristics of porcine gastric slow wave activity determined by high-resolution mapping. Neurogastroenterol Motil. 2010; 22:e292–e300. [PubMed: 20618830]
25. Angeli TR, Cheng LK, Du P. Loss of interstitial cells of Cajal and patterns of gastric dysrhythmia in chronic unexplained nausea and vomiting (CUNV). Gastroenterology. 2015; 149:56–66. [PubMed: 25863217]
26. Ladabaum U, Koshy SS, Woods ML, Hooper FG, Owyang C, Hasler WL. Differential symptomatic and electrogastrographic effects of distal and proximal human gastric distension. Am J Physiol. 1998; 275(3 Pt 1):G418–G424. [PubMed: 9724252]
27. O'Grady G, Paskaranandavadivel N, Angeli TR, Du P, Windsor JA, Cheng LK, Pullan AJ. A comparison of gold versus silver electrode contacts for high-resolution gastric electrical mapping using flexible printed circuit board arrays. Physiol Meas. 2011; 32:N13–N22. [PubMed: 21252419]
28. Yassi R, O'Grady G, Paskaranandavadivel N, Du P, Angeli T, Pullan A, Cheng L, Erickson J. The gastrointestinal electrical mapping suite (GEMS): software for analyzing and visualizing high-resolution (multi-electrode) recordings in spatiotemporal detail. BMC Gastroenterol. 2012; 12:60. [PubMed: 22672254]
29. Paskaranandavadivel N, O'Grady G, Du P, Cheng LK. Comparison of filtering methods for extracellular gastric slow wave recordings. Neurogastroenterol Motil. 2013; 25:79–83. [PubMed: 22974243]
30. Erickson J, O'Grady G, Du P. Falling-edge, variable threshold (FEVT) method for the automated detection of gastric slow wave events in serosal high-resolution electrical recordings. Ann Biomed Eng. 2010; 38:1511–1529. [PubMed: 20024624]
31. Erickson J, O'Grady G, Du P, Egbuji J, Pullan A, Cheng L. Automated cycle partitioning and visualization of high-resolution activation time maps of gastric slow wave recordings: the Region Growing Using Polynomial Surface-estimate stabilization (REGROUPS) Algorithm. Ann Biomed Eng. 2011; 39:469–483. [PubMed: 20927594]
32. Weeks, M. Digital signal processing using matlab and wavelets. Second. London: Jones and Bartlett Publishers; 2010.
33. Paskaranandavadivel N, Cheng L, Du P, O'Grady G, Pullan A. Improved signal processing techniques for the analysis of high resolution serosal slow wave activity in the stomach. Conf Proc IEEE Eng Med Biol Soc. 2011:1737–1740. [PubMed: 22254662]
34. Paskaranandavadivel N, O'Grady G, Du P, Pullan A, Cheng L. An improved method for the estimation and visualization of velocity fields from gastric high-resolution electrical mapping. IEEE Trans Biomed Eng. 2012; 59:882–889. [PubMed: 22207635]
35. Bayly P, KenKnight BH, Rogers J, Hillsley RE, Ideker R, Smith W. Estimation of conduction velocity vector fields from epicardial mapping data. IEEE Trans Biomed Eng. 1998; 45:563–571. [PubMed: 9581054]
36. Du P, Wenlian Q, O'Grady G, Egbuji JU, Lammers W, Cheng LK, Pullan AJ. Automated detection of gastric slow wave events and estimation of propagation velocity vector fields from serosal high-resolution mapping. Conf Proc IEEE Eng Med Biol Soc. 2009:2527–2530. [PubMed: 19964973]
37. Angeli T, Du P, Paskaranandavadivel N, Janssen PW, Beyder A, Lentle RG, Bissett IP, Bissett Ian P, Cheng LK, O'Grady G. The bioelectrical basis and vadility of gastrointestinal extracellular slow wave recordings. J Physiol. 2013; 591:4567–4579. [PubMed: 23713030]
38. Miedema BW, Sarr MG, Kelly KA. Pacing the human stomach. Surgery. 1992; 111:143–150. [PubMed: 1736383]
39. O'Grady G, Du P, Lammers WJ, Egbuji JU, Mithraratne P, Chen JD, Cheng LK, Windsor JA, Pullan AJ. High-resolution entrainment mapping of gastric pacing: a new analytical tool. Am J Physiol Gastrointest Liver Physiol. 2010; 298:G314–G321. [PubMed: 19926815]

40. Du P, Hameed A, Angeli TR, Lahr C, Abell TL, Cheng LK, O'Grady G. The impact of surgical excisions on human gastric slow wave conduction, defined by high-resolution electrical mapping and in silico modeling. Neurogastroenterol Motil. 2015; 27:1409–1422. [PubMed: 26251163]

41. Lerouge S, Tabrizian M, Wertheimer MR, Marchand R, Yahia LH. Safety of plasma-based sterilization: Surface modifications of polymeric medical devices induced by Sterrad and Plazlyte™ processes. Biomed Mater Eng. 2002; 12:3–13. [PubMed: 11847405]

42. Yin J, Chen JDZ. Electrogastrography: methodology, validation and applications. J Neurogastroenterol Motil. 2013; 19:5–17. [PubMed: 23350042]

43. Bradshaw LA, Irimia A, Sims JA, Gallucci MR, Palmer RL, Richards WO. Biomagnetic characterization of spatiotemporal parameters of the gastric slow wave. Neurogastroenterol Motil. 2006; 18:619–631. [PubMed: 16918726]

44. Cheng LK, O'Grady G, Du P, Egbuji JU, Windsor JA, Pullan AJ. Gastrointestinal system. Wiley Interdisciplinary Reviews: Systems Biology and Medicine. 2010; 2:65–79. [PubMed: 20836011]

45. Paskaranandavadivel N, Wang R, Sathar S, O'Grady G, Cheng LK, Farajidavar A. Multi-channel wireless mapping of gastrointestinal serosal slow wave propagation. Neurogastroenterol Motil. 2015; 27:580–585. [PubMed: 25599978]

46. Ver Donck L, Lammers WJEP, Moreaux B, Smets D, Voeten J, Vekemans J, Schuurkes JAJ, Coulie B. Mapping slow waves and spikes in chronically instrumented conscious dogs: implantation techniques and recordings. Med Biol Eng Comput. 2006; 44:170–178. [PubMed: 16937158]

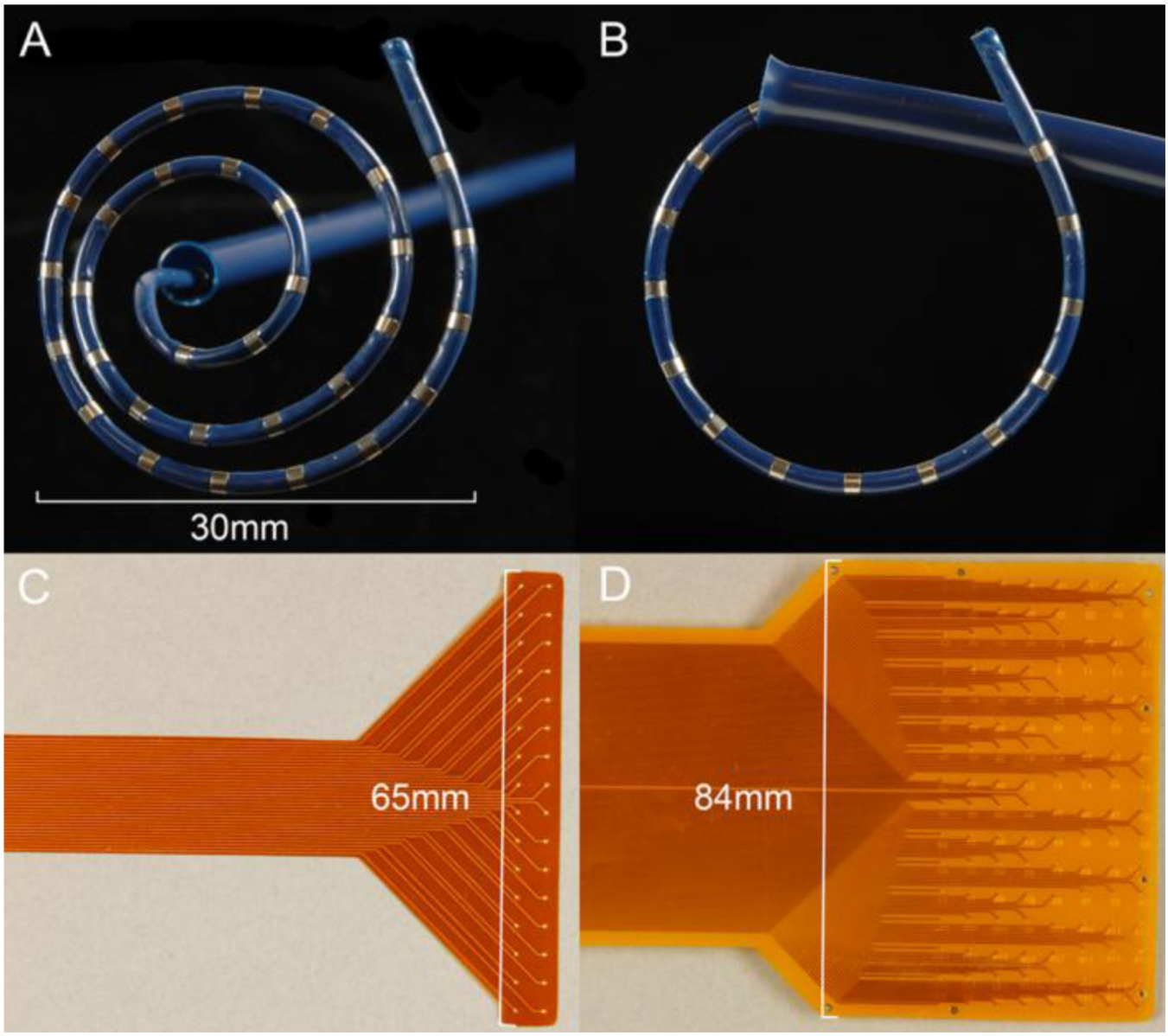

Figure 1.

Novel and reference electrode devices. **A, B**. The novel laparoscopic device, shown with the recording tip fully deployed (**A**) and partially retracted (**B**). The flexible recording catheter of the laparoscopic device (diameter 2.2 mm, length 330 mm) can be readily passed through a 5 mm laparoscopic port. The head consists of 32 recording channels in a spiral arrangement (5 mm spacing) that is positioned against the serosa for data collection. **C, D.** Reference flexible printed circuit board arrays used for device validation. Two configurations were used: **(C)** A 32 channel array (4 × 8 electrodes; 4 mm spacing); and **(D)** a 128 channel array (16 × 8 electrodes, 5.2 mm spacing).

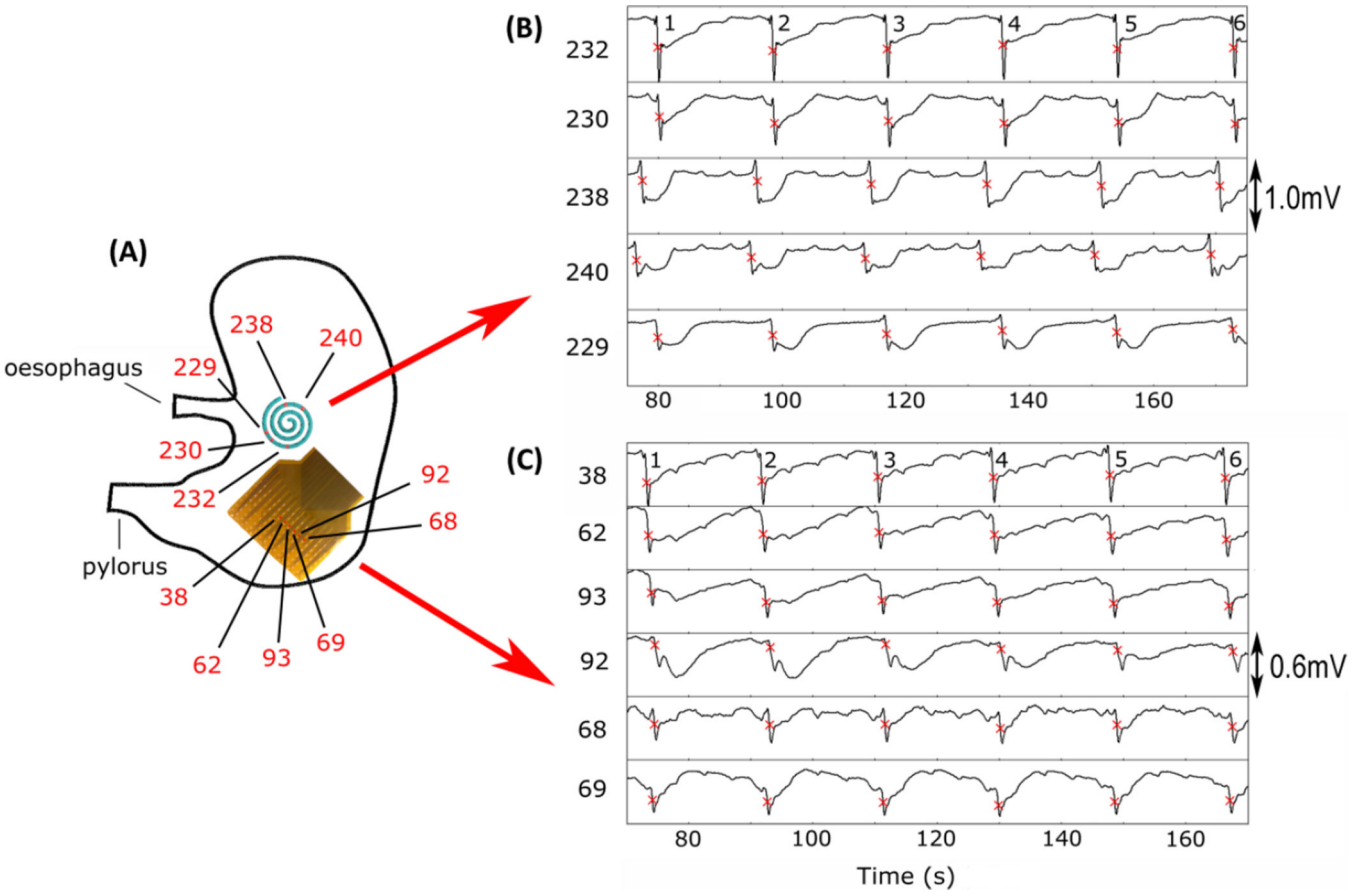

Figure 2.

Example electrode traces from the laparoscopic and reference electrodes. **(A)** Positioning of a reference electrode (128 electrodes in total; 360 mm^2) and the laparoscopic device (32 electrodes in total; 707 mm^2) on the stomach during data collection. **(B)** The electrograms for five recording channels from the laparoscopic device, and six from the reference array are displayed along with their locations on the electrode arrays. The electrograms demonstrate consistent aboral slow wave activity, with six events occurring within the displayed period of 90 seconds for both the laparoscopic device and reference electrode (frequency: 2.6 ± 0.3 cpm vs 2.5 ± 0.5 cpm).

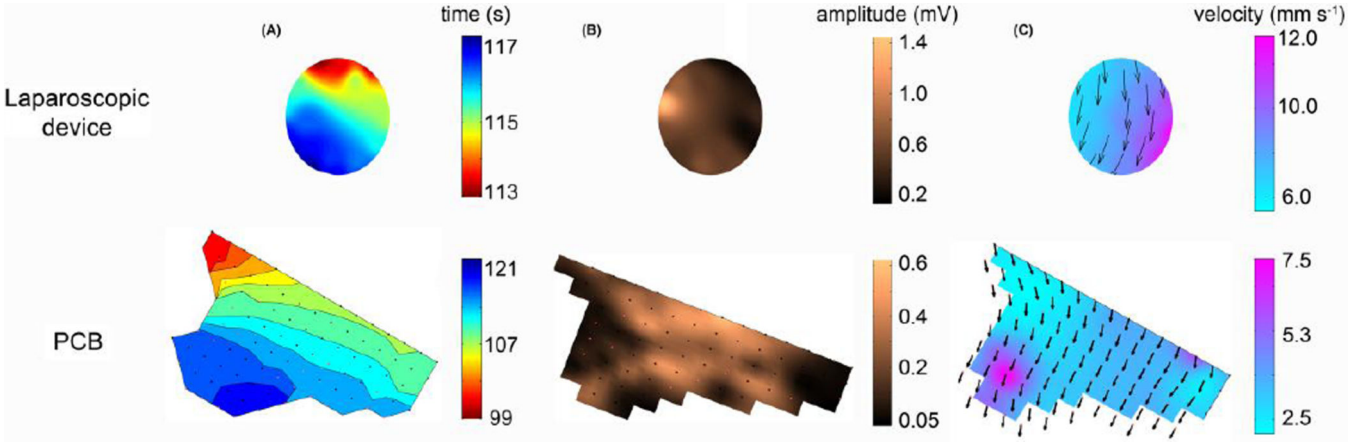

Figure 3.

Activation time, amplitude and velocity maps constructed using data from the same slow wave event for the laparoscopic device and reference electrode array. The electrode positioning relates to those indicated in Figure 2. Velocity is represented by arrows and color field indicating magnitude of speed (cyan slowest speed and purple highest speed).The maps in this example indicate that both the laparoscopic device and reference electrodes have recorded consistent propagation in an aboral direction. The 8 second delay visible in the registration of slow wave activity between the laparoscopic device and the reference array can be attributed to the distance between the recording devices during data collection (see Figure 2).

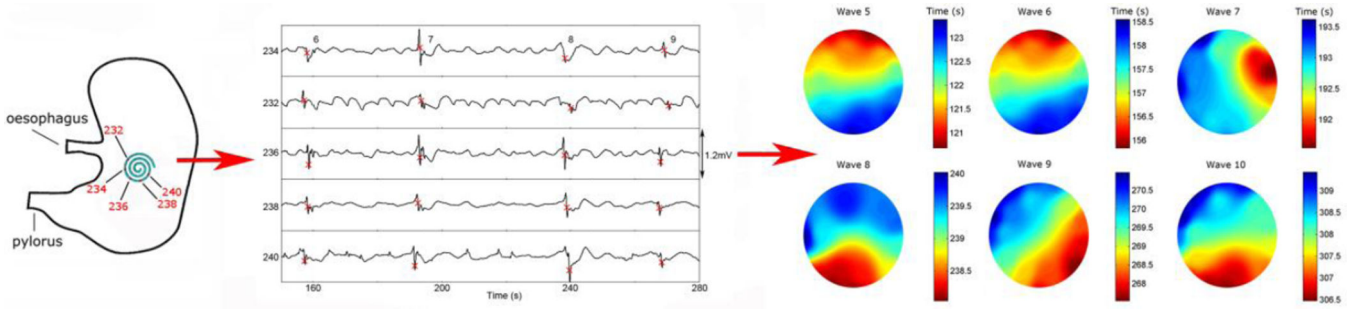

Figure 4.

Example of dysrhythmic activity captured using the laparoscopic device. **(A)** Positioning of the device on the stomach during data collection. **(B)** The electrograms recorded from five electrodes (numbers displayed), with four slow wave events occurring within the displayed period of 120 seconds (frequency 1.4 ± 0.5 cpm). **(C)** The resultant activation maps demonstrate the dysrhythmic activity in the form of a deviation in direction from aboral, to circumferential, to orad over the course of five slow wave events.

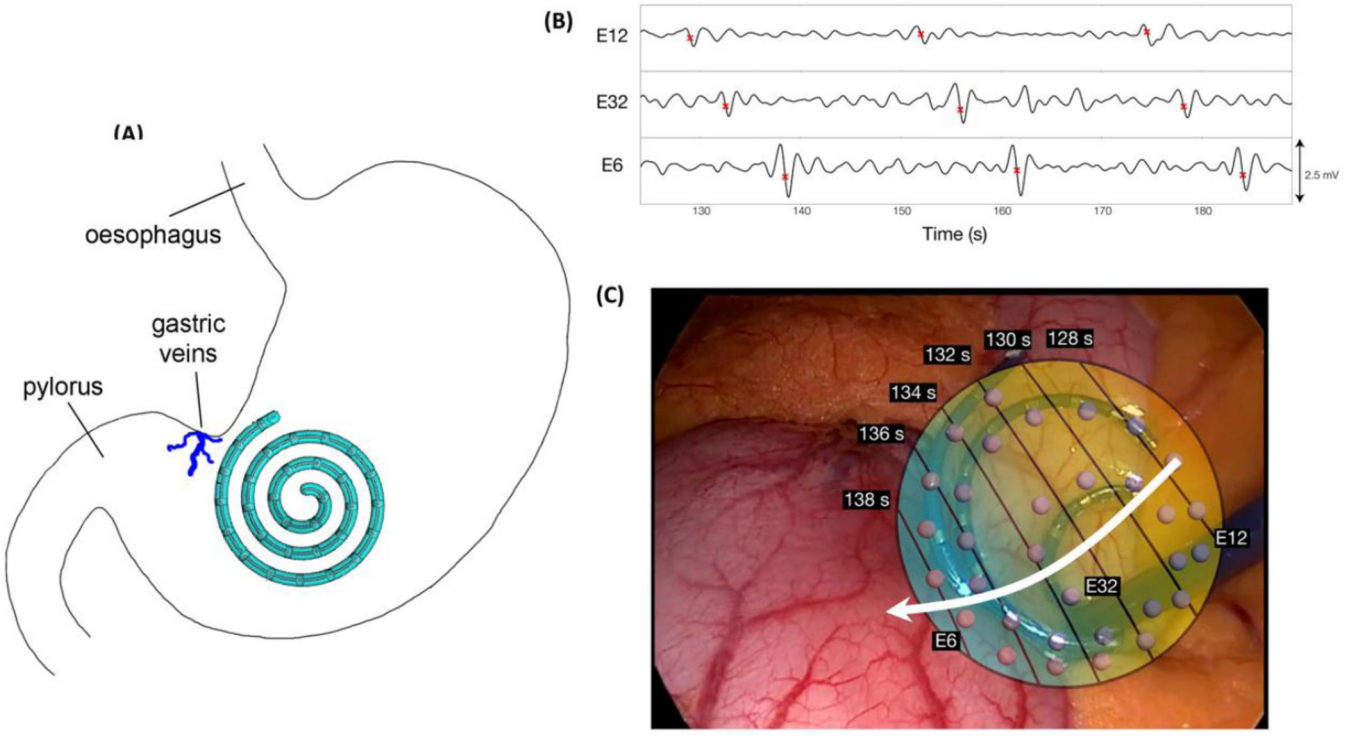

Figure 5.

Example electrode traces and AT map constructed from human intraoperative data. **(A)** Positioning of the laparoscopic device on the stomach during data collection. **(B)** The electrograms from three recording channels (numbers displayed), with three slow wave events occurring within the displayed period of 60 seconds (frequency 2.7 ± 0.03 cpm). **(C)** The resultant activation map has been overlayed on an interoperative image of the laparoscopic device. The electrode positioning relates to that indicated in *A*. The white arrow indicates the direction of the propagating slow waves in an aboral direction.

Table 1

Comparison of slow wave characteristics between the laparoscopic device and reference electrode array.

	Laparoscopic Device	**Reference Electrode Array**	***p-value***
Frequency (cpm)	2.5 ± 0.4	2.6 ± 0.4	0.91
Amplitude (mV)	1.3 ± 0.1	1.4 ± 0.1	0.4
Signal to Noise Ratio (dB)	17.5 ± 0.65	12.8 ± 0.60	<0.001
Velocity (mm s^{-1})	8.9 ± 0.2	8.7 ± 0.1	0.2